



Using a local Monte Carlo strategy to assess 1-D velocity models from wide-angle seismic travel-time data and application to the Rockall Trough

S. Pearce^{a,1}, R. Hobbs^{b,*}, M. Bosch^c

^a Department of Earth Sciences, University of Cambridge, CB3 0EZ, UK

^b Department of Earth Sciences, University of Durham, DH1 3LE, UK

^c Department of Applied Physics, Universidad Central de Venezuela, Caracas, Venezuela

ARTICLE INFO

Article history:

Received 21 March 2007

Received in revised form 23 June 2008

Accepted 15 July 2008

Available online 27 July 2008

Keywords:

Seismic modelling
Travel-time inversion
Uncertainty

ABSTRACT

We present a statistically based search strategy to explore velocity–depth model space derived from the inversion of seismic refraction and wide-angle data. The method is based on the Metropolis algorithm and computes the likelihood of any given model of fitting the observed data. By iteratively perturbing the model, the model space is sampled and the resulting probability density function provides a quantified measure of the velocity resolution as a function of depth. Unlike manual analysis, where a single layer is perturbed to test its sensitivity ignoring the effect on the deeper layers, this method computes the fit for the whole model at each iteration and only selects the models that achieve a specified global fit. We show results of the algorithm from the 1-D inversion of Expanding Spread Profiles from the central part of the Rockall Trough to the west of Britain. As expected, the method highlights the areas of the model that are both well and poorly constrained and shows the degradation of resolution with increasing depth such that for high quality data the accumulated velocity errors at basement depths is $\pm 5\%$. This error increases as the data quality decreases and the estimated pick error increases.

© 2008 Elsevier B.V. All rights reserved.

1. Introduction

The use of long-offset seismic data to define the velocity structure of the sub-surface is well established (Cerveny and Psencik, 1984; Fuchs and Müller, 1971; Hole et al., 2005; Mereu, 1990; Zelt and Smith, 1992). In areas where little lateral variation is expected, e.g. along strike or in the centre of basins, two ships can be used to create a synthetic super gather called an Expanding Spread Profile (ESP) (Musgrave, 1962). The cost of this method is high compared to using OBS/H and analysis is restricted to 1-D but the advantage of this method is data redundancy which enables stacking of common offset data to improve the signal-to-noise ratio yielding long-offset dataset of the highest quality.

Analysis of long-offset data usually involves three steps: data processing and geometry assignment; identification of individual phases, picking their travel time versus offset, and estimation of picking error; and inversion of the travel-time data to give the optimum velocity model. Additional modelling and perturbation of target layers are used to assess the sensitivity of the parts of the model and its overall resolution. RAYINVR (Zelt and Smith, 1992) is an extensively used code that has been well tested and is accepted as a

benchmark that can invert both reflection and refraction data. The user provides the observed picked travel times and a velocity versus depth model. The code computes the forward data from the model and compares it to the observed data. By iteratively updating the model the error is reduced until an acceptable misfit (χ^2) is obtained. A satisfactory model will give a χ^2 close to one, which means the fit of the computed data to the observed data is similar to the original picking errors of the observed data. It is normal practice to trade the χ^2 value against model complexity to establish the minimum acceptable geological structure that adequately fits the data.

Unfortunately this inversion problem is non-unique and there is a family of models that would fit the data within acceptable limits. The arrival at the particular final model is dependent on several factors, these include: the quality of the data, which has a finite bandwidth and contains noise; the total number of sources and receivers and their layout; and how the model is parametrised. Even with high quality data, it is likely that the same data analysed using a different inversion scheme or with a different strategy will produce a different result; they will be similar in the gross sense but not in the detail. To manually explore the range of potential models would be time consuming so testing is normally restricted to a number of key layers and resolution analysis using checker-board patterns (Zelt and Smith, 1992; Zelt, 1999). An alternative approach is to use a 'Monte Carlo' based method many random models are generated and compared to find a best fitting range of parameters; or we could take a model and perturb it systematically to find out how well resolved each of the

* Corresponding author.

E-mail address: r.w.hobbs@durham.ac.uk (R. Hobbs).

¹ Present address. Chevron Energy Technology Company, Houston, TX 77002, USA.

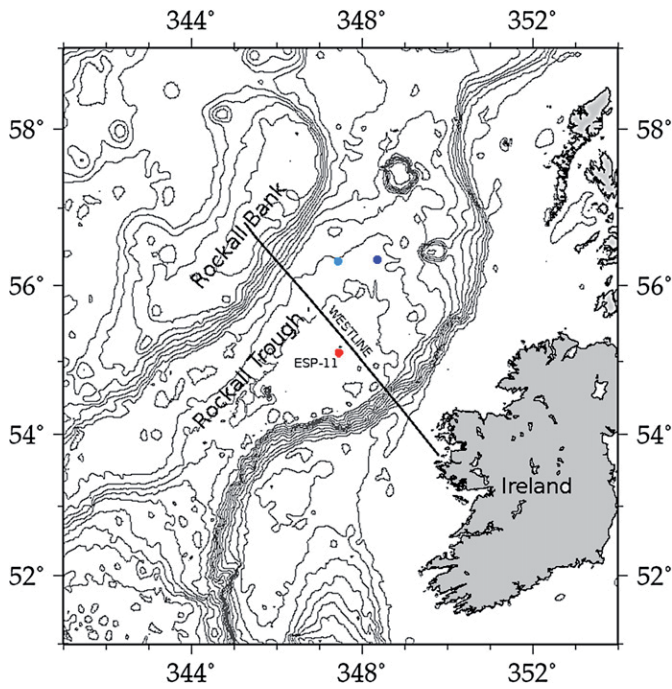


Fig. 1. Locations of ESPs in central Rockall Trough. Red circle, ESP-11; dark blue circle, ESP 89-1; and light blue circle, ESP 87-1. The black line is the location of the BIRPS WESTLINE deep seismic profile (England, 1995).

model parameters are. By filtering the results to give models that have a χ^2 below a certain value and specifying that they must reach above a set percentage of picks, we can begin to find a set of models that are acceptable. Either of the methods would, eventually, both find the optimum model and also quantify the uncertainty for each of the parameters. However, they are both computationally expensive and many of the generated models would fail or be geologically unlikely, though this could be addressed by placing bounds on the model space. In this paper we assume the solution from an inversion is acceptable,

Table 1

Table of picked phases from ESP-11 together with the results from the inversion.

Identifier	Colour	Phase	N_{pts}	T_{rms} (s)	χ^2
1	Light blue	Sea-floor reflection	285	0.032	0.279
2	Green	Upper sedimentary reflection 1	116	0.005	0.066
3	Green	Upper sedimentary reflection 2	142	0.013	0.407
4	Green	Upper sedimentary reflection 3	34	0.003	0.022
5	Green	Lower sedimentary reflection 1	81	0.008	0.177
6	Green	Lower sedimentary reflection 2	64	0.012	0.337
7	Yellow	Possible basement reflection	158	0.011	0.283
8	Red	Crustal reflection	130	0.024	0.160
9	Dark blue	Moho reflection	222	0.028	0.019
10	Green	Upper sedimentary refraction 1	30	0.005	0.054
11	Green	Lower sedimentary refraction 1	23	0.004	0.041
12	Green	Lower sedimentary refraction 2	57	0.008	0.178
13	Yellow	Possible crustal refraction 1	31	0.017	0.086
14	Red	Possible crustal refraction 2	93	0.015	0.022
Total		Whole model	1466	0.021	0.182

N_{pts} is the number of picks fitted, T_{rms} is rms time misfit, and χ^2 is the normalised ratio of the time misfit to estimated pick error for each phase and for the whole model. The colours are used in Fig. 2 to highlight the interpreted reflection and refractions.

in that it is geologically plausible and fits the data to an acceptable level, and we want to test uncertainty of this model against the original data rather than the much larger question of whether the inversion solution is the best possible model. To achieve this aim, we use a Markov Chain based method called the Metropolis algorithm (Metropolis et al., 1953) to investigate the shape of the inversion objective function in the vicinity of our solution as a statistically robust approach. To avoid introducing possible systematic errors in changing the forward modelling algorithm and associated parameterisation we use those provided by the RAYINVR code.

To test our approach we inverted some ESP data from the Rockall trough (Fig. 1) to the west of the British Isles to derive a velocity–depth mode. The central area of the Rockall trough is characterized by flat laying sediments over a basement with little apparent relief (England and Hobbs, 1997). So provide an ideal target for ESP surveys. High redundancy, high spatial sampling and a repeatable seismic air-gun source mean that these data can be processed and stacked to give a

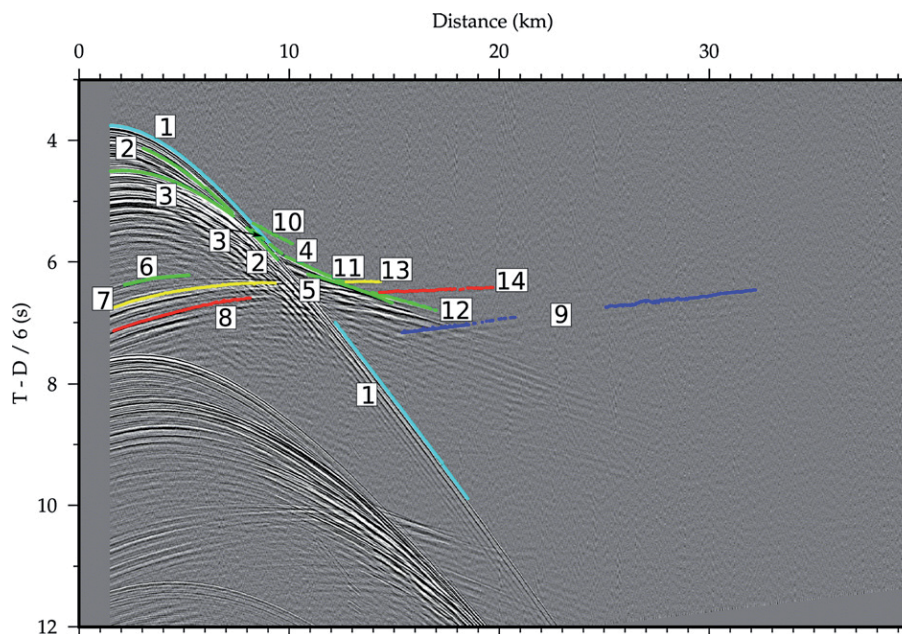


Fig. 2. ESP-11 after signature deconvolution and showing picks used in the RAYINVR inversion. The colours and numbers of the picks correspond to the phases listed in Table 1. Gather plotted with a reduction velocity of 6 km/s.

long-offset common mid-point gather with a high signal to noise. These data (ESP-11) were previously analysed by Joppen and White (1990). For this work we reprocessed the data which included estimation of the signal source and deterministic deconvolution to maximise temporal bandwidth and minimise picking uncertainty (Fig. 2). Fourteen possible phases were identified which constrained a twelve layer model with either a reflected arrival, a refracted arrival or both. Using RAYINVR a velocity–depth profile was computed that fitted the observed data (Table 1, Fig. 3). Comparison with other results are shown (Joppen and White, 1990; Hobbs and Collier, 1997) and, as expected, the gross structure is similar but the detail is different.

2. Metropolis–Hastings algorithm

Mosegaard and Tarantola (1995) and more recently Mosegaard and Sambridge (2002) present the Bayesian based Metropolis algorithm that provably samples the a posteriori probability density using Markov chain Monte Carlo methods as a means to assess uncertainty in inverse problems. The algorithm consists of two parts. The first part randomly perturbs a model which is then passed to the second part of the algorithm which decides if the model passes a data fitting test. An iteration of the algorithm is as follows: a selected parameter is perturbed from the current model (m_{cur}) to form a new model (m_{new}), the likelihood is calculated, and the m_{new} is accepted or rejected according to a set of simple rules:

- 1) if the value of the likelihood $L(m_{\text{new}})$ of the new model is larger than or equal to the likelihood $L(m_{\text{cur}})$ of the current model, m_{new} is accepted;
- 2) if the difference in the exponent of the likelihood function (defined below) for m_{new} from the equivalent exponent of the starting model is greater than a threshold value, m_{new} is rejected;

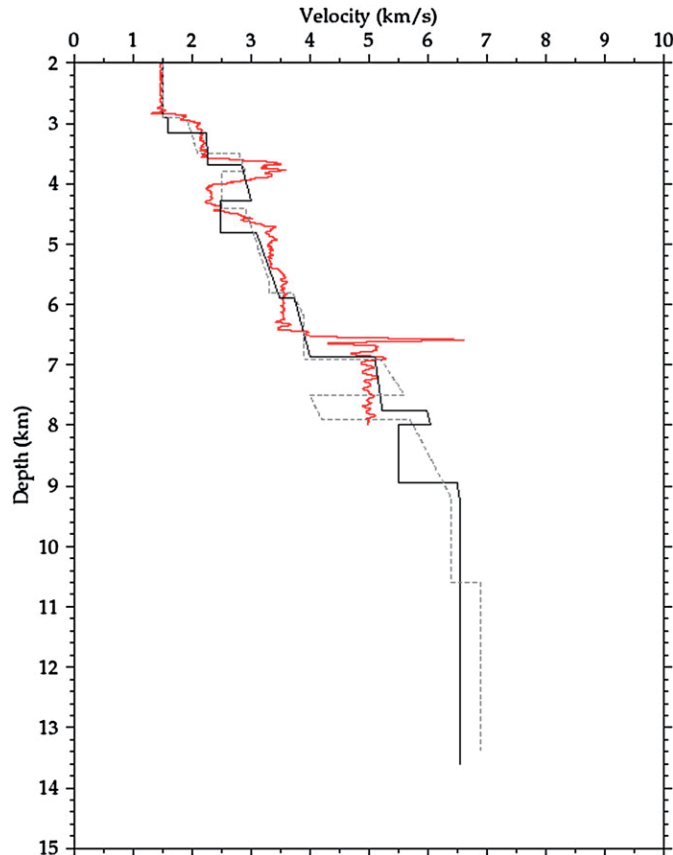


Fig. 3. Comparison three results for ESP-11. Dashed line, Joppen and White (1990); red line, Hobbs and Collier (1994); solid line, Pearce (2002).

- 3) if the value of $L(m_{\text{new}})$ is smaller than $L(m_{\text{cur}})$, then a random decision to accept m_{new} is made, with the probability $L(m_{\text{new}})/L(m_{\text{cur}})$ of accepting m_{new} , otherwise m_{new} is rejected.

In the cases (2) and (3) if the m_{new} is rejected then the model reverts to m_{cur} and a new random perturbation is proposed.

In the RAYINVR inversion code (Zelt and Smith, 1992), and other similar ray-tracing algorithms, a normalised misfit χ^2 value is computed to indicate the goodness of a fit between calculated and observed travel times. Which is expressed as

$$\chi^2 = \frac{1}{N-1} \sum_{i=1}^N \frac{(t_i^{\text{cal}} - t_i^{\text{obs}})^2}{\sigma_i^2} \quad (1)$$

where N is the number of observed picks predicted by the model; t^{cal} and t^{obs} are the calculated and observed travel times for pick i respectively; and σ_i is the standard deviation, or estimate of the travel-time uncertainty, of that pick. For large N , when the difference between the observed and calculated travel time approaches the uncertainty then χ^2 approaches 1.0.

An alternative approach is to calculate a model likelihood. By comparing the likelihoods of two or more models we can draw similar conclusions about their relative fit. A likelihood can be calculated using the multivariate Gaussian distribution

$$L'(m) = (2\pi)^{-\frac{N}{2}} \prod_{i=1}^N (\sigma_i^{-1}) \exp \left[-\frac{1}{2} \sum_{i=1}^N \frac{(t_i^{\text{cal}} - t_i^{\text{obs}})^2}{\sigma_i^2} \right]. \quad (2)$$

We can relate the χ^2 value returned by RAYINVR by combining Eq. (1) and Eq. (2). Also if N , in Eq. (2), were a constant then we can replace the product in the equation with a constant c given that the pick uncertainty is estimated from the observed data (Pearse, 2002) to get

$$L'(m) = c \times \exp \left[-\frac{1}{2} (N-1) \chi^2 \right]. \quad (3)$$

N can be considered as a constant only if the forward modelling produces a calculated travel time for every observed pick from the real data, i.e. there is a t^{cal} for every t^{obs} . However, in complex models the number of t^{cal} for a phase and the range over which it can be observed may change for each model for example: changes in velocity gradient in a layer can shift arrivals to a different offset range that does not match the observed data; or a velocity drop across a boundary can lose some or all arrivals from the layers below. To enable the simplification in Eq. (3) we use the number of observations (t^{obs}) which always remains constant. Unfortunately this will favour models with a low χ^2 irrespective of whether or not all of the observed picks are reached by the calculated phase. So a model that produces theoretical travel times that fit the observed data well but for only a minority of the observed picks so will be preferred over a model that produces theoretical travel times with a reasonable fit for the majority of the observed picks. In order for latter model to be considered more probable, it is necessary to weight the outcome so that the likelihood is bias towards fitting more data at the expense of χ^2 . For mathematical convenience we choose this “hit-rate” function such that our final likelihood for a given model m is

$$L(m) = c \times \exp \left(-\frac{1}{2} \left[(N^{\text{obs}} - 1) \chi^2 + (N^{\text{obs}} - N^{\text{cal}})^2 \right] \right). \quad (4)$$

where N^{cal} and N^{obs} are the number of calculated and observed picks. The selection of the hit-rate function, $(N^{\text{obs}} - N^{\text{cal}})^2$, is arbitrary and determined by trial and error. The number of missed picks squared was found to be satisfactory for the case in hand. If the impact of this function

on the likelihood is too small, the search will accept models that do not predict a significant number of the observed picks, in the limit the likelihood reverts to Eq. (3). If it is too large then the converse occurs and the search is dominated by models that predict all the data irrespective of the misfit with the observed travel times. To avoid the likelihood of the perturbed model getting too small, a threshold is set such that the exponent in Eq. (4) should not be more than given value from the original model from the inversion. This value has to be tuned to reflect what would be a minimum acceptable hit-rate and maximum misfit. Unlike prior which should not be data dependent, this effects the computed likelihood which is a function of how well particular parameters fit the data. So the effect is to modify the likelihood by setting it to zero for any model that exceeds the threshold.

By restricting ourselves to a 1-D model the total number of model parameters is small and because of the data quality the total number of observations is high. These combine to give a well constrained likelihood function so it was not necessary to impose any restrictions on the prior model space other than a threshold on the exponent. However, for less well constrained likelihood functions it may be necessary to impose some prior conditions to particular layers to ensure the search remains in parts of the model space that are geologically plausible.

3. Model perturbation

To achieve a statistically robust estimate of the uncertainty, it is necessary to create a sufficient number of perturbed models that efficiently sample the model space. The input files for RAYINVR define each layer as a depth to the top of the layer in kilometres, and the velocity at the top and bottom of the layer in kilometres per second. This parameterisation means that layer thickness, mean velocity and gradient are all strongly linked. If we perturb the depth to the top of a layer then we are changing the thickness and velocity gradient of this layer and the layer immediately above, or if we perturb either the upper or lower velocity within a layer we will change the mean velocity and gradient for the travel time of the this layer and all the subsequent layers. In either case the perturbed model will probably only achieve a low likelihood because the misfit for all the subsequent picks will increase and it will probably fail the threshold test or, given the rules above, be rejected making the search inefficient. Our observations are measured in time so in the depth–velocity domain, the possible range of solutions will lie along the diagonal (Fig. 4a) for pre-critical reflections where there is a trade-off between interface depth and over-burden velocity structure. By transforming the model

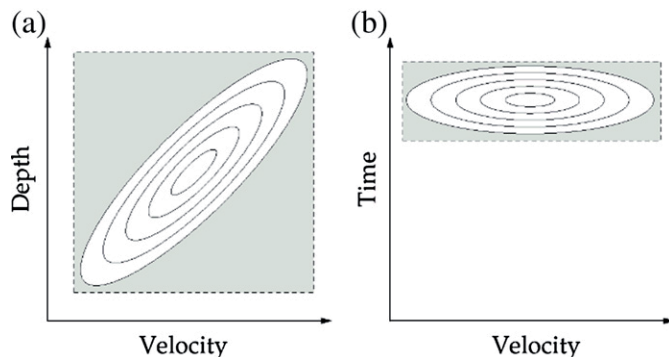


Fig. 4. A schematic of the relationship of near-normal incidence travel-time observations plotted in (a) depth–velocity domain and (b) time–velocity domain. The ellipses represent the likelihood function given a level of uncertainty in the travel-time pick. If the two parameters are perturbed independently then the square boxes on each plot represents the range of values that need to be sampled to adequately describe the possible uncertainty. The gray area represents the unacceptable models. By using the time–velocity domain the area of unacceptable models is significantly reduced so the Metropolis–Hastings search will be more efficient. For refracted arrivals the major axis of the likelihood contours would be rotated in the direction of the velocity axis because refracted arrivals are more sensitive to velocity than depth.

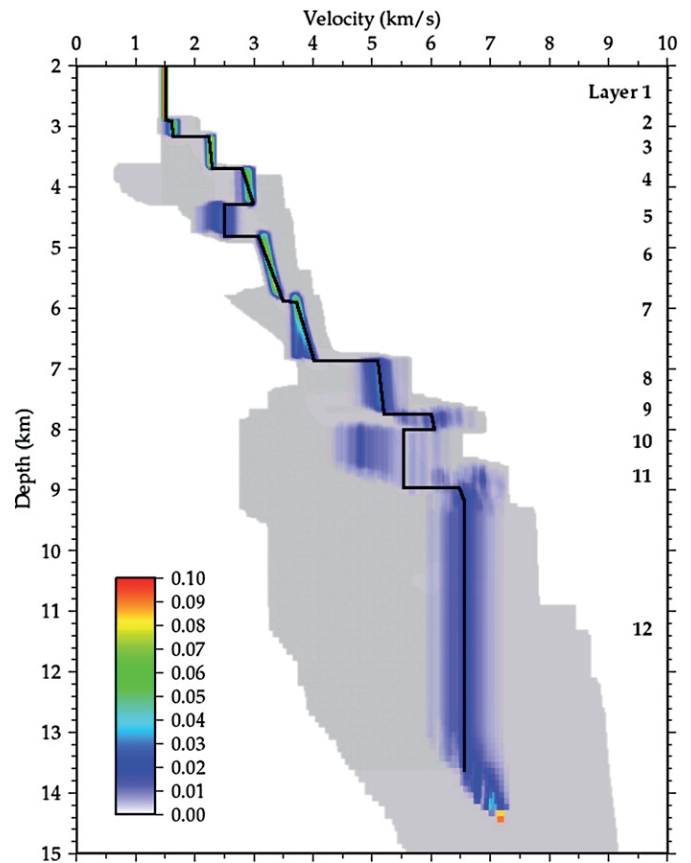


Fig. 5. Probability density functions of the velocity with depth for ESP-11. This distribution was calculated after 20,000 iterations of the Metropolis code, the range of models sampled is enclosed by the grey area. The coloured velocity posteriori probability density function has been normalized at each depth interval. Beneath the well resolved water layer are three sediment layers with increasing velocities (layers 2, 3 and 4). The layer 3 has a smaller range of velocities (0.2 km/s) than the layers above and below (0.3–0.4 km/s). The layer 5 (4.2–4.8 km) does not have an average velocity constrained by a turning ray with velocities for this layer is controlled by the fit of a reflection from the base of the layer. Layer 6 (4.8–5.8 km) is well constrained with pronounced velocity gradient. Between layers 7 and 8 there is a significant velocity step below this step velocity is less well constrained particularly layer 10.

from the depth–velocity domain to the time–velocity domain (Fig. 4b) we can reparameterise each layer in the model by normal incidence travel time, mean velocity and velocity gradient. Now for each layer we can vary the velocity gradient and, by linking any changes in mean velocity to a corresponding change in thickness, vary mean velocity without significantly changing the travel time. So perturbations in either of these parameters will not cause a major change in the misfit for subsequent layers. The layer thickness is only affected by perturbing the normal incidence travel time and, because of the reasons stated above, is the most sensitive. After perturbation we convert the model into the format required by RAYINVR.

A starting model and a set of travel-time picks is given to the program. The program then calculates the travel times and misfit using RAYINVR. The likelihood is calculated using Eq. (4). At each iteration of the algorithm, a layer is chosen at random and one of the corresponding model parameters (mean velocity, velocity gradient, and normal incidence travel time) is modified by adding a random perturbation pulled from a uniform probability function. The likelihood for the new model is calculated and it is accepted or rejected according to the rules above. This process continues for a given number of iterations, in this case a total of 20,000. This number is chosen to be large so it gives the algorithm enough iterations to investigate the model space and give a robust posteriori probability density function (PDF). This function is calculated for each depth by

Table 2

Comparison by layer of the velocity from the original inversion result with the mean and variance determined from the Metropolis search.

Layer	Name	Constraining phases (refraction and reflection from base)	Sample depth (km)	Velocity from inversion (km/s)	Mean velocity (km/s)	Variance (km/s)
1	Sea water	1	2.5	1.50	1.50	0.02
2	Upper sedimentary layer	2	3.0	1.60	1.66	0.08
3	Upper sedimentary layer	3	3.4	2.26	2.26	0.04
4	Upper sedimentary layer	10	4.0	2.92	2.91	0.08
5	Upper sedimentary layer	4	4.5	2.48	2.44	0.24
6	Lower sedimentary layer	5, 11	5.4	3.29	3.29	0.07
7	Lower sedimentary layer	6, 12	6.4	3.87	3.83	0.08
8	Lower sedimentary layer ?	7	7.3	5.17	5.10	0.22
9	Crustal layer ?	13	7.9	6.01	6.06	0.50
10	Crustal layer ?	8	8.5	5.50	4.79	0.36
11	Crustal layer	14	9.1	6.53	6.59	0.30
12	Crustal layer	9	11.4	6.55	6.57	0.24

For most layers the agreement is good except for layer 10 where the mean velocity is lower than the inversion result.

gridding the accepted models with a resolution of 0.01 km in depth and 0.01 km/s in velocity and counting the number of times the accepted velocity models passed through each grid cell. The bin-width is chosen to convey the uncertainty at any part of the model at a useful scale and retain subtle variations of the distributions.

4. Application of the metropolis method to real data

The objective is to quantify the uncertainty in a given model rather than the larger issue of finding the optimum model. So we are assuming the given model, derived using an accepted ray-tracing approach, satisfies the requirements of fit to the data and geological plausibility. The travel-time picks, their uncertainty and their phase assignment were taken from this given model and subjected to the Metropolis method described above. For our data the threshold condition for acceptance (rule 2 above) was set to 1400. This represents a maximum allowable loss in the number of observed picks fitted by a model of 38 compared with the final RAYINVR inversion result. This represents 2.5% of the total number of picks. The resulting PDF is shown in Fig. 5. A qualitative assessment gives the

expected results that the model is less well resolved with depth and low velocity layers are less well resolved. Table 2 gives the results of the analysis for the centre of each layer against the original model. The agreement is good and, for all but one layer, the original model velocity is within one standard deviation of the mean of the posteriori PDF. The exception is layer 10, a low velocity layer, which is constrained only by pre-critical reflections so there is a trade-off between velocity and thickness. The inversion gave an acceptable result for a 950 m thick layer with a velocity of 5.50 km/s whereas the Metropolis search prefers a 820 m thick layer with a velocity of 4.79 km/s. Overlaying this model on a nearby WESTLINE (England, 1995) seismic reflection profile (Fig. 6) (Pearse, 2002) shows this layer incorporates a bright reflection that is interpreted as a sill intrusion. This thin layer is not detected in the wide-angle data though it does have a strong influence on the full-waveform inversion of the pre-critical data (Hobbs and Collier 1997) (Fig. 3). Examination of the variance shows that the uncertainty is high for the low velocity layers (5,10), where there is no reflection from the layer base to help constrain the velocity (layer 12) and where the layers are thin (9,11).

5. Conclusions

The statistically based resolution analysis presented in this paper represents a significant development on the current practice of manual perturbations of single layers that ignores the knock-on effects on fit of other parts of the model. The output plots give an assessment of how the picked data constrains the model and can possibly identify over- or under-parameterisation. Though individual iterations are quick it is necessary to run several thousand models to obtain a meaningful result. We demonstrate the method on ESP data acquired over in the centre of the Rockall trough where sediment structure is consistent with the 1-D assumption inherent in the ESP method. This type of data was chosen as it is the simplest to invert as it imposes this 1-D restriction which limits the number of model parameters. Given this assumption we conclude that even with the highest quality ESP data, the error on the travel-time picks is sufficient to introduce uncertainty of typically 5% in the final model.

The key step in formulating the Metropolis algorithm for this type of data is redefining the misfit parameter (χ^2) to be weighted by the total number of observed picks for a given phase rather than the number of picks fitted which is model dependent.

For the simple 1-D model presented here we computed 20,000 iterations to constrain 24 parameters (12 layers), so approximately 1000 iterations per parameter. For more complex models, e.g. 2-D, the number of parameters will increase. This would require a similar increase in the number of iterations required to compute a robust posteriori PDF. As the run-time for each iteration is largely determined by the time taken to forward trace the rays through the model the total time would also be a function of the number of shots and

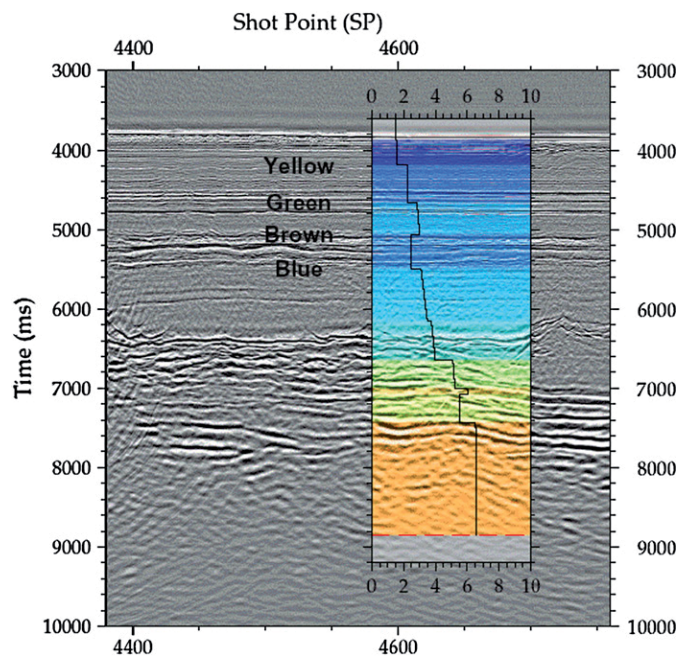


Fig. 6. ESP-11 velocity model projected onto WESTLINE deep seismic reflection profile (see Fig. 1 for location). Velocities shown are in km/s. The key reflectors labeled are based on Masson and Kidd (1986) as extrapolated onto WESTLINE by England and Hobbs (1997).

receivers in the dataset. This increase in total time maybe partly addressed by imposing prior conditions which would need to be taken into account when interpreting the posterior PDF. For 2-D models interpretation of the determined uncertainty is also more complex and will include errors introduced by unconstrained lateral variation in velocity either in the original data or model parameterisation.

Acknowledgments

RWH is a NERC Advanced Research Fellow (NER/J/S/2002/00745), the research was done by SP as part of a studentship at Cambridge funded by Isle of Man Government, Department of Education, collaboration with MB was while he was working with the LITHOS project at Cambridge funded by Isle of Man Government, Department of Education. The authors thank Florian Bleibinhaus and one other reviewer for constructive comments.

References

- Cerveny, V., Psencik, I., 1984. SEIS83-numerical modeling of seismic wave-field in 2-D laterally varying layered structures by ray method. In: Engdahl, E.R. (Ed.), *Documentation of Earthquake Algorithms*, number Rep. SE- 35. World Data Center (A) for Solid Earth Geophysics, Boulder, Colorado, pp. 36–40.
- England, R.W., 1995. Westline: a deep near-normal incidence reflection profile across the Rockall Trough. In: Croker, P.F., Shannon, P.M. (Eds.), *The Petroleum Geology of Ireland's Offshore Basins*, Special Publication 93. The Geological Society, London, pp. 423–427.
- England, R.W., Hobbs, R.W., 1997. The structure of the Rockall Trough imaged by deep seismic reflection profiling. *J. Geol. Soc. London* 154 (3), 497–502.
- Fuchs, K., Müller, G., 1971. Computation of synthetic seismograms with the reflectivity method and comparison with observation. *Geophys. J. R. Astron. Soc.* 23, 417–433.
- Hobbs, R.W., Collier, J., 1997. The 1-D full-waveform inversion of a common mid-point gather with a known source function. In: Snyder, D.B., Warner, M.R. (Eds.), *Journal of Conference Proceedings*, 1. Cambridge Publications, pp. 21–28. Commission on Controlled Source Seismology.
- Hole, J.A., Zelt, C.A., Pratt, R.G., 2005. Advances in controlled-source seismic imaging. *Eos. Trans. Amer. Geophys. Union* 86, 177, 181.
- Joppen, M., White, R.S., 1990. The structure and subsidence of Rockall Trough from two-ship seismic experiments. *J. Geophys. Res.* 95 (B12), 19821–19837.
- Masson, D.G., Kidd, R.B., 1986. Revised Tertiary seismic stratigraphy of the southern Rockall Trough. In: Ruddiman, W.F., Kidd, R.B., Thomas, E., et al. (Eds.), *Initial reports of the Deep Sea Drilling Project covering Leg 94, 94*. U.S. Govt. Printing Office, pp. 1117–1126.
- Metropolis, N., Rosenbluth, A.W., Rosenbluth, M.N., Teller, A.H., Teller, E., 1953. Equation of state calculations by fast computing machines. *J. Chem. Phys.* 1 (6), 1087–1092.
- Mosegaard, K., Tarantola, A., 1995. Monte Carlo sampling of solutions to inverse problems. *J. Geophys. Res.* 100 (B7), 12431–12447.
- Mosegaard, K., Sambridge, M., 2002. Monte Carlo analysis of inverse problems. *Inverse Probl.* 18, R29–R54 1.
- Mereu, R.F., 1990. The complexity of the crust from refraction/wide-angle reflection data. *Pure Appl. Geophys.* 132, 269–288.
- Musgrave, A.W., 1962. Applications of the expanding reflection spread. *Geophysics* 27, 981–993.
- Pearse, S. (2002). PhD Dissertation Cambridge.
- Zelt, C.A., 1999. Modelling strategies and model assessment for wide-angle seismic traveltimes data. *Geophys. J. Int.* 139, 183–204.
- Zelt, C.A., Smith, R.B., 1992. Seismic travel time inversion of 2-D crustal velocity structure. *Geophys. J. Int.* 108, 16–31.